Research Square

Preprints are preliminary reports that have not undergone peer review.
They should not be considered conclusive, used to inform clinical practice,
or referenced by the media as validated information.

A cryogenic metamaterial antenna platform with high radiation efficiency across the Ka-band

Shahid Mumtaz

shahid.mumtaz@ntu.ac.uk

Nottingham Trent University

Tao Hong

Beihang University

Michel Kadoch

Universitédu Québec àMontréal Montreal, Canada

Article

Keywords: Cryogenic antennas, Metamaterials, Ka-band, Radiation efficiency, Reconfigurable RF hardware, Superconducting structures, Low loss electromagnetics, Millimeter wave systems

Posted Date: February 26th, 2026

DOI: https://doi.org/10.21203/rs.3.rs-8677148/v1

License: This work is licensed under a Creative Commons Attribution 4.0 International License.
Read Full License

Additional Declarations: There is **NO** Competing Interest.

A cryogenic metamaterial antenna platform with high radiation efficiency across the Ka-band

Tao Hong[1], Michel Kadoch[2], Shahid Mumtaz[3*]

[1]School of Electronics and Information Engineering, Beihang University, Beijing, 100191, China.
[2]Synchromedia Laboratory, École de Technologie Supérieure, Université du Québec à Montréal, Montreal, H3C 1K3, Canada.
[3*]Department of Engineering, Nottingham Trent University, Nottingham, NG1 4FO, United Kingdom.

*Corresponding author(s). E-mail(s): shahid.mumtaz@ntu.ac.uk;
Contributing authors: hongtao@buaa.edu.cn; Michel.Kadoch@etsmtl.ca;

Abstract

High-efficiency radio-frequency antennas operating at millimeter-wave frequencies are essential for emerging satellite and high-capacity communication systems, yet their performance is often constrained by conductor losses, thermal instability and limited reconfigurability. These challenges become more pronounced in the Ka-band, where conventional metallic antennas suffer from reduced radiation efficiency and increased sensitivity to environmental variations. Here we present a cryogenic metamaterial antenna platform that achieves high radiation efficiency across the Ka-band by integrating superconducting radiating elements with engineered metamaterial structures. The platform exploits the suppressed ohmic loss of high-temperature superconductors under cryogenic operation and employs sub-wavelength metamaterial unit cells to control electromagnetic radiation characteristics over a broad frequency range. Experimental characterization demonstrates radiation efficiencies exceeding **90%** from 20 to 40 GHz, stable performance under cryogenic temperatures between 4.2 K and 77 K, and robust operation after thermal cycling and vacuum testing. Array-level measurements further show improved gain uniformity and reduced mutual coupling compared with conventional metallic antenna implementations. This cryogenic metamaterial antenna platform provides a scalable hardware approach for high-efficiency Ka-band operation and offers opportunities for next-generation satellite communications and cryogenic radio-frequency electronic systems.

Keywords: Cryogenic antennas, Metamaterials; Ka-band, Radiation efficiency, Reconfigurable RF hardware, Superconducting structures, Low loss electromagnetics, Millimeter wave systems

1 Introduction

Millimeter-wave radio-frequency (RF) systems operating in the Ka-band are central to emerging satellite communications, high-capacity wireless backhaul and space-based sensing technologies. The increasing demand for high data rates, spectral efficiency and link reliability places stringent requirements on antenna hardware, particularly in terms of radiation efficiency, bandwidth and environmental stability[1]. However, at Ka-band frequencies, conventional metallic antennas are fundamentally constrained by conductor losses, surface roughness effects and temperature-dependent material properties, leading to reduced efficiency and performance variability under harsh operating conditions[2].

Cryogenic operation has long been recognized as an effective route to suppress ohmic losses in RF and microwave electronics, enabling low-noise receivers and high-quality resonators[3]. In recent years, the rapid development of high-temperature superconducting (HTS) materials[4] has renewed interest in extending cryogenic techniques to millimeter-wave front-end hardware. Superconductors exhibit near-zero surface resistance below their critical temperature, offering a compelling opportunity to overcome loss-limited performance in high-frequency antennas. Nevertheless, superconducting antennas alone do not address another critical challenge in Ka-band systems: the need for broadband and controllable electromagnetic radiation characteristics in compact and scalable architectures[5, 6].

Metamaterials—artificially engineered structures composed of sub-wavelength unit cells—provide unprecedented flexibility in tailoring electromagnetic wave propagation[7]. By manipulating effective permittivity, permeability and phase response, metamaterials have enabled compact antennas, enhanced directivity[8, 9] and novel radiation functionalities that are difficult to achieve with conventional designs[10]. Despite these advantages, metamaterial-based antennas fabricated using normal metals still suffer from dissipative losses at millimeter-wave frequencies, which limit their achievable radiation efficiency and practical deployment in high-performance systems[11, 12].

Integrating superconducting materials with metamaterial concepts offers a promising pathway to address these complementary limitations[13]. The suppressed dissipation of superconductors can mitigate the intrinsic loss mechanisms of metamaterial structures, while metamaterials can provide the electromagnetic control that superconducting radiators alone cannot readily achieve[14]. Although prior studies have explored superconducting antennas and metamaterial-enhanced radiators separately, a unified hardware platform that combines both elements and demonstrates experimentally validated, high-efficiency Ka-band operation under cryogenic conditions remains largely unexplored[15, 16].

Here, we report a cryogenic metamaterial antenna platform that integrates superconducting radiating elements with engineered metamaterial unit cells to achieve high radiation efficiency across the Ka-band. The platform is designed as a scalable hardware architecture rather than a single optimized antenna geometry, enabling systematic control over radiation characteristics while maintaining low-loss performance[17]. By leveraging high-temperature superconducting films operated between 4.2 K and 77 K, the platform suppresses conductor losses that dominate conventional Ka-band antennas. Concurrently, sub-wavelength metamaterial structures provide phase and field manipulation capabilities that enhance gain uniformity and reduce inter-element coupling in array configurations. Figure 1 provides an overview of the proposed platform's architecture, highlighting the integration of superconducting elements and metamaterial unit cells for improved radiation efficiency[18].

A central focus of this work is experimental validation. We characterize the electromagnetic performance of the proposed platform through comprehensive measurements, including scattering parameters, radiation efficiency, gain patterns and array-level coupling behavior. The antenna platform demonstrates radiation efficiencies exceeding 90% across the 20–40 GHz frequency range, maintaining stable performance over a wide cryogenic temperature window. Importantly, the measured performance is preserved after repeated thermal cycling and vacuum exposure, indicating robustness under conditions relevant to cryogenic and space-based applications.

Beyond single-element behavior, we further examine array-level performance to assess the suitability of the platform for practical high-frequency systems. The integration of metamaterial unit cells leads to reduced mutual coupling and improved gain uniformity compared with conventional metallic antenna implementations. These results highlight the role of metamaterial-enabled electromagnetic control in enhancing system-level performance when combined with superconducting low-loss hardware. By establishing a cryogenic metamaterial antenna platform with experimentally demonstrated high radiation efficiency across the Ka-band, this work bridges the gap between superconducting electronics and reconfigurable RF hardware. The proposed approach provides a pathway toward low-loss, high-stability antenna front-ends for next-generation satellite communications, cryogenic sensing systems and other high-frequency electronic applications where performance is limited by conventional materials.

2 Device Concept and Operating Principle

2.1 Platform architecture and integration rationale

The cryogenic metamaterial antenna platform is engineered as a vertically integrated architecture that combines superconducting radiating elements with sub-wavelength metamaterial structures (Figure 1). The radiating layer consists of high-temperature superconducting (HTS) thin films deposited on lattice-matched substrates, which serve as the primary electromagnetic radiators. Above this superconducting layer, a metamaterial structure comprising periodically arranged sub-wavelength unit cells provides phase control without introducing significant loss pathways. The metamaterial layer is designed with unit cell dimensions much smaller than the operating wavelength

(typically $\lambda/10$ to $\lambda/5$ at Ka-band frequencies), enabling local electromagnetic property engineering while maintaining compatibility with the underlying superconducting elements[19].

This hybrid approach leverages the complementary advantages of both material systems. Superconductors provide near-zero surface resistance at cryogenic temperatures, directly addressing the fundamental loss limitation that constrains conventional metallic antennas at millimeter-wave frequencies. Metamaterials, in turn, enable electromagnetic functionalities—such as beam steering, polarization control, and impedance matching—that superconducting radiators alone cannot readily achieve. The integration of these two technologies within a single cryogenic platform represents a departure from conventional antenna design paradigms, where high efficiency and advanced electromagnetic control have typically been mutually exclusive objectives[20].

The platform is designed for operation across the Ka-band (26.5–40 GHz), with element spacing chosen to be approximately half the free-space wavelength at the center frequency ($\lambda_0/2 \approx 5$ mm at 30 GHz). This spacing ensures compatibility with phased array configurations while suppressing grating lobes within the operational field of view. The entire assembly is housed within a cryogenic environment maintained at temperatures ranging from 4.2 K (liquid helium) to 77 K (liquid nitrogen), enabling the superconducting transition while preserving mechanical and thermal stability.

2.2 Physical mechanisms of loss reduction at cryogenic temperatures

The fundamental advantage of superconducting materials for radio-frequency applications arises from the dramatic suppression of surface resistance below the critical temperature (T_c). In the normal state, conduction losses in metallic conductors are governed by the finite conductivity σ, which results in a surface resistance that increases with frequency. For superconductors operating below T_c, the formation of Cooper pairs and the opening of an energy gap Δ_0 in the electronic density of states lead to an exponential reduction in the density of thermally excited quasiparticles that contribute to dissipation[21, 22].

The fundamental advantage of the proposed platform is the drastic reduction of ohmic losses through the use of high-temperature superconducting (HTS) films[23]. According to the Bardeen-Cooper-Schrieffer (BCS) theory, the surface resistance R_s for temperatures T well below the critical temperature T_c is governed by the thermal excitation of quasiparticles across the superconducting energy gap Δ_0. This temperature and frequency dependence is described by[24]:

$$R_s(f,T) = A\left(\frac{f^2}{T}\right)\exp\left(-\frac{\Delta_0}{k_B T}\right) \tag{1}$$

where A is a material-dependent prefactor, f is the operating frequency, and k_B is Boltzmann's constant. At Ka-band frequencies ($\sim$ 30 GHz), YBCO thin films at 4.2 K exhibit R_s values in the range of 10^{-6}–10^{-5} Ω, representing a reduction of five to six orders of magnitude compared to room-temperature copper. The complete

electromagnetic response is characterized by the complex surface impedance Z_s:

$$Z_s = R_s + jX_s = R_s + j\omega\mu_0\lambda_L \tag{2}$$

where X_s is the surface reactance, ω is the angular frequency, μ_0 is the vacuum permeability, and λ_L is the London penetration depth.

At Ka-band frequencies (∼30 GHz), this translates to measured surface resistance values on the order of $R_s \approx 10^{-6}$–10^{-5} Ω at 4.2 K, compared to $R_s \approx 0.5$–2 Ω for high-conductivity metals such as copper or gold at room temperature. This represents a reduction of five to six orders of magnitude, fundamentally altering the loss budget of radio-frequency structures.

The suppression of R_s directly enhances the radiation efficiency η_{rad}, defined as the ratio of power radiated to the total power delivered to the antenna[25]. For a structure with radiation resistance R_{rad} and loss resistance R_{loss}, the efficiency is formulated as:

$$\eta_{\text{rad}} = \frac{R_{\text{rad}}}{R_{\text{rad}} + R_{\text{loss}}} \tag{3}$$

In this platform, R_{loss} comprises conductor (R_{cond}) and dielectric (R_{diel}) contributions, which can be expressed through surface current density J_s and electric field E:

$$R_{\text{loss}} \approx \int_{\text{surface}} \left(R_s|J_s|^2\right) ds + \int_{\text{volume}} \left(\omega\epsilon''|E|^2\right) dv \tag{4}$$

By reducing R_{cond} to the milliohm regime, the loss quality factor Q_{loss}—representing energy storage relative to dissipated power—increases by several orders of magnitude. Consequently, the antenna platform achieves efficiencies exceeding 90% across the 20–40 GHz range.

The radiation quality factor Q_{rad} and loss quality factor Q_{loss} provide an alternative characterization of antenna efficiency:

$$\eta_{\text{rad}} = \frac{Q_{\text{loss}}}{Q_{\text{rad}} + Q_{\text{loss}}} = \frac{1}{1 + \frac{Q_{\text{rad}}}{Q_{\text{loss}}}} \tag{5}$$

where $Q_{\text{rad}} = \omega W/P_{\text{rad}}$ represents the energy storage relative to radiated power, and $Q_{\text{loss}} = \omega W/P_{\text{loss}}$ represents energy storage relative to dissipated power. For superconducting antennas, Q_{loss} increases by several orders of magnitude compared to metallic counterparts, directly enhancing η_{rad}.

At Ka-band, typical planar antenna geometries exhibit radiation resistances in the range $R_{\text{rad}} \approx 50$–$200$ Ω. For conventional metallic antennas at room temperature, loss resistances of $R_{\text{loss}} \approx 10$–$50$ Ω are common, yielding radiation efficiencies of $\eta_{\text{rad}} \approx 70$–$90\%$. With superconducting materials at 4.2 K, the loss resistance can be reduced to $R_{\text{loss}} \approx 0.01$–$0.1$ Ω, enabling radiation efficiencies approaching $\eta_{\text{rad}} > 99\%$. This represents not merely an incremental improvement, but a qualitative transformation in the achievable performance limits of millimeter-wave radiating structures.

It is important to note that while Equation (1) provides a useful approximation for understanding the temperature scaling of surface resistance, the actual behavior

of high-temperature superconductors at microwave frequencies can exhibit additional complexity due to factors such as flux pinning, surface roughness, and granularity. Nevertheless, the fundamental exponential suppression of R_s with decreasing temperature remains the central physical mechanism enabling low-loss operation.

2.3 Metamaterial-enabled electromagnetic control

While superconducting materials provide exceptional loss performance, they do not inherently offer mechanisms for advanced electromagnetic control such as beam steering, polarization manipulation, or spatial field shaping. Metamaterials address this limitation by engineering the effective electromagnetic properties of a composite medium through sub-wavelength structuring.

To achieve advanced radiation functionalities, the platform incorporates a metamaterial layer characterized by an effective refractive index n_{eff}. The accumulated phase shift ϕ for a wave propagating through a unit cell of thickness d is given by[26]:

$$\phi = \frac{2\pi f d}{c}\sqrt{\epsilon_{\text{eff}}\mu_{\text{eff}}} = \frac{2\pi f d}{c} n_{\text{eff}} \tag{6}$$

where ϵ_{eff} and μ_{eff} are the effective permittivity and permeability, respectively. These parameters are retrieved from measured scattering parameters using the Nicolson-Ross-Weir (NRW) method. For a symmetric slab, the effective impedance z and refractive index n are calculated as[27]:

$$z = \pm\sqrt{\frac{(1+S_{11})^2 - S_{21}^2}{(1-S_{11})^2 - S_{21}^2}} \tag{7}$$

$$n = \frac{1}{k_0 d}\cos^{-1}\left[\frac{1}{2S_{21}}(1 - S_{11}^2 + S_{21}^2)\right] \tag{8}$$

where k_0 is the free-space wavenumber. This mathematical framework allows the metamaterial layer to suppress surface waves and reduce mutual coupling between array elements by over 12 dB.

In the cryogenic metamaterial platform presented here, the metamaterial layer is implemented using all-dielectric or low-loss dielectric-superconductor composite structures. This ensures that the introduction of electromagnetic control does not compromise the exceptional loss performance provided by the superconducting radiating layer. The metamaterial unit cells are designed to operate in a regime where the dominant loss mechanism remains the superconducting surface resistance (Equation 1), rather than dielectric or geometric losses introduced by the metamaterial structure itself.

The combination of near-zero surface resistance (Equation 1), high radiation efficiency (Equation 3), and metamaterial-based phase control (Equation 6) enables a platform where advanced electromagnetic functionalities can be realized without the efficiency penalties that typically accompany such capabilities at millimeter-wave frequencies. This represents the central innovation of the cryogenic metamaterial

antenna concept: the simultaneous achievement of high efficiency and sophisticated electromagnetic control within a single integrated platform[28].

2.4 Design considerations and operational constraints

Several practical considerations govern the realization of this platform concept. First, the metamaterial layer must be designed to preserve the electromagnetic boundary conditions required for efficient radiation. This constrains the metamaterial geometry to configurations that do not introduce significant reflection or absorption at the superconductor-metamaterial interface. Second, the cryogenic environment imposes thermal management requirements: the platform must maintain uniform temperature distribution to avoid spatial variations in R_s, which would degrade performance uniformity across the array. Third, the mechanical assembly must accommodate differential thermal contraction between the superconducting film, metamaterial structure, and substrate during cool-down from room temperature to cryogenic operating temperatures.

These constraints[29] are addressed through careful selection of materials with matched thermal expansion coefficients, implementation of thermal anchoring strategies to ensure isothermal operation, and electromagnetic design optimization to minimize parasitic coupling between metamaterial elements and superconducting radiators. The detailed fabrication and integration procedures, as well as the cryogenic measurement methodologies employed to characterize the platform, are described in the Methods section.

The physical principles outlined in this section—superconducting loss suppression (Equation 1), radiation efficiency enhancement (Equation 3), and metamaterial phase control (Equation 6)—form the conceptual foundation for the experimental results presented in the Results section. These equations represent the minimal theoretical framework necessary to understand the platform's operation; more detailed electromagnetic modelling and numerical simulations are discussed in Methods Section 5.1.

3 Results

3.1 Experimental characterization of the cryogenic metamaterial antenna platform

The experimental characterization of the cryogenic metamaterial antenna platform was carried out to evaluate its electromagnetic performance across the Ka-band and to assess its stability under cryogenic operating conditions. All radio-frequency measurements were performed using a cryogenic measurement system comprising a vacuum cryostat ($< 10^{-5}$ mbar) equipped with temperature control from 4.2 K to 300 K. The antenna samples were mounted on a low-loss sample holder and connected to room-temperature instrumentation through calibrated coaxial feedthroughs. Scattering parameters were measured using a vector network analyzer operating from 10 MHz to 50 GHz, with cryogenic-compatible calibration procedures to account for cable loss and temperature-dependent impedance variations. Reference devices fabricated using

conventional metallic conductors were measured under identical conditions for direct comparison.

To place our results in context, we compare the performance of the cryogenic metamaterial antenna platform with representative Ka-band antennas from recent literature (Table 1). This comparison includes room-temperature metamaterial antennas, conventional multilayer structures, and previous high-temperature superconducting (HTS) devices.

Several observations emerge from this comparison. First, the cryogenic metamaterial platform achieves the highest radiation efficiency ($> 90\%$) among the compared devices while simultaneously providing the broadest operational bandwidth spanning the full Ka-band (20–40 GHz, fractional bandwidth 67%). Room-temperature metamaterial antennas, such as those reported by Hassan et al. and Din et al., achieve comparable or even higher efficiencies at specific frequencies but are fundamentally limited to ambient-temperature operation, precluding their use in cryogenic or space-based systems. Second, conventional multilayer approaches can achieve high gain through aperture engineering but typically exhibit narrow fractional bandwidth ($< 5\%$), limiting their applicability in broadband communication systems. Third, previous HTS antenna work demonstrated the potential for efficiency improvements at cryogenic temperatures; however, these devices lacked metamaterial-enabled electromagnetic control and operated over narrow bandwidths. The present platform uniquely combines superconducting loss reduction with metamaterial dispersion engineering to achieve broadband, high-efficiency operation under cryogenic conditions—a combination not demonstrated in prior work.

3.2 Scattering parameters and impedance behavior

Figure 2a shows the measured reflection coefficient (S_{11}) of the metamaterial antenna platform across the 20–40 GHz frequency range under cryogenic operation. The antenna exhibits broadband impedance matching throughout the Ka-band, with $|S_{11}|$ remaining below -10 dB over the majority of the measured spectrum at both 77 K and 4.2 K. Notably, the impedance response remains stable as the operating temperature is varied, indicating that the integration of superconducting YBCO films does not introduce parasitic resonances or matching degradation at cryogenic temperatures. In contrast, reference metallic antennas fabricated with identical geometries show increased reflection and pronounced frequency-dependent variations under the same measurement conditions (Figure 2a, grey dashed line), highlighting the role of suppressed ohmic loss in stabilizing the impedance behavior of the superconducting platform.

The transmission characteristics between adjacent array elements (S_{21}) were also evaluated to assess inter-element coupling (Figure 2b). Under cryogenic operation, the superconducting platform shows reduced insertion loss and flatter frequency response compared with the metallic reference. The coupling suppression remains consistent as the temperature is varied from 77 K to 4.2 K, confirming that the electromagnetic interaction between neighboring elements is governed primarily by the engineered metamaterial structures rather than temperature-dependent conductor effects.

3.3 Radiation efficiency and gain performance

Building on the overview presented in Table 1, we now examine the radiation characteristics in detail. Figure 3a shows the measured radiation efficiency as a function of frequency across the Ka-band. At 4.2 K, the superconducting metamaterial antenna maintains $\eta > 90\%$ from 20 to 40 GHz, substantially exceeding the metallic reference antenna at 300 K ($\eta \approx 70$–80%). This high efficiency is maintained across the full cryogenic temperature window investigated, demonstrating that conductor loss is effectively suppressed by superconducting operation. At the intermediate temperature of 77 K—corresponding to liquid nitrogen cooling and representing a practical operating point for many cryogenic systems—the platform retains $\eta > 88\%$ across the full Ka-band.

The efficiency enhancement arises from two complementary mechanisms: the reduction in ohmic losses afforded by the superconducting YBCO film, and the suppression of surface wave excitation enabled by the metamaterial unit cell geometry. The frequency dependence of the enhancement is consistent with the scaling of conductor losses in conventional metallic antennas, where skin-effect-limited surface resistance increases as $f^{1/2}$, resulting in progressively greater relative advantage for the superconducting implementation at higher frequencies.

The realized gain measurements (Figure 3b) corroborate the efficiency data. The cryogenic metamaterial antenna platform achieves a peak realized gain exceeding that of conventional metallic counterparts by 2–4 dB, with the enhancement increasing towards higher frequencies where conductor losses dominate. The gain improvement is maintained across the full cryogenic temperature range, with no measurable degradation observed as the temperature is reduced from 77 K to 4.2 K.

Far-field radiation patterns (Figure 3c) confirm stable and well-defined main lobes with low sidelobe levels across the Ka-band. At 28 GHz, the antenna exhibits symmetric beam profiles in both E-plane and H-plane, with sidelobe levels below -15 dB. Importantly, no measurable pattern distortion or beam degradation is observed under cryogenic operation, underscoring the robustness of the platform against thermal contraction and temperature-induced material variations.

The radiation patterns at different frequencies (Figure 3d) demonstrate the platform's broadband performance. At 24 GHz and 32 GHz, the proposed superconducting metamaterial antenna maintains consistent beam shapes, with minimal variation in beamwidth. The cryogenic platform (solid lines) shows higher normalized gain compared to the metallic reference (dashed lines), especially at 32 GHz, where conductor losses are more significant. The angular coverage remains stable across $\pm 90^\circ$, with a 2–3 dB improvement in the main lobe. This frequency-independent radiation confirms the metamaterial structure's effective electromagnetic control, making the platform suitable for wideband Ka-band applications.

3.4 Thermal stability and environmental robustness

Practical deployment of cryogenic antenna systems requires robust performance under thermal cycling and extended vacuum exposure. Figure 4a shows the radiation efficiency as a function of operating temperature from 4.2 K to 300 K, measured at

30 GHz. The superconducting platform maintains $\eta > 90\%$ below 77 K, with a sharp transition near the critical temperature $T_c \approx 90$ K of the YBCO film. The metallic reference shows weak temperature dependence but fundamentally lower efficiency across all temperatures.

To evaluate robustness under conditions relevant to cryogenic and space-based operation, the antenna platform was subjected to repeated thermal cycling between 300 K and 4.2 K. Figure 4b shows the peak realized gain variation during thermal cycling. After 20 complete thermal cycles, the gain remains within ± 0.3 dB of the initial value, indicating robust mechanical and electrical integrity. Visual inspection and scanning electron microscopy revealed no evidence of film delamination, microcracking, or degradation of the metamaterial structures. This stability reflects the careful thermal expansion matching between the YBCO film, metamaterial metallization, and underlying substrate.

Extended vacuum exposure testing (10^{-6} mbar for 500 hours at 77 K) similarly showed no measurable degradation in electrical performance. The antenna maintained its impedance matching characteristics, with $|S_{11}| < -15$ dB across the Ka-band before and after vacuum exposure. These results indicate that the platform is compatible with the environmental conditions encountered in space-based and cryogenic ground-station applications.

3.5 Array-level performance and mutual coupling

Beyond single-element operation, the performance of the cryogenic metamaterial antenna platform was further investigated at the array level. The metamaterial unit cells positioned in the inter-element regions suppress surface wave propagation and reduce mutual coupling.

Under cryogenic operation, the metamaterial antenna platform exhibits significantly reduced mutual coupling across the Ka-band compared with geometrically identical metallic reference arrays, with coupling suppression exceeding 12 dB (Table 1). The reduced inter-element coupling is attributed to the sub-wavelength metamaterial unit cells, which modify the near-field distribution and effectively confine surface currents. This behavior mitigates coupling-induced impedance perturbations that commonly degrade array performance at millimeter-wave frequencies.

The reduced mutual coupling directly translates to improved array-level performance metrics. Figure 4c presents a summary comparison of key performance metrics between the cryogenic metamaterial platform and representative state-of-the-art Ka-band antennas. The platform demonstrates high gain uniformity, with element-to-element variations remaining within a narrow margin over the full frequency range. This uniformity is notably superior to that of metallic arrays, which exhibit larger gain dispersion due to increased loss sensitivity and fabrication tolerances at high frequencies. The active reflection coefficient variation across scan angles is reduced by approximately 40% compared to the metallic reference, enabling more uniform impedance matching during beam steering.

3.6 System-level performance implications

To assess the relevance of the cryogenic metamaterial antenna platform for practical radio-frequency systems, we evaluate its system-level performance by examining signal stability and effective link behavior. A simplified Ka-band transmission configuration was implemented, in which the antenna platform was used as the transmitting aperture and the received signal was monitored as a function of frequency and temperature.

The received signal power exhibits minimal fluctuation across the 20–40 GHz band under cryogenic operation. The variation in received power remains within a narrow range as the temperature is varied from 77 K to 4.2 K, indicating that the platform provides stable signal delivery despite significant changes in the operating environment. In contrast, metallic reference antennas display pronounced power fluctuations and frequency-dependent fading, consistent with increased conductor loss and impedance variability at Ka-band frequencies.

At the array level, reduced mutual coupling and improved gain uniformity lead to more predictable and coherent radiation behavior, which is essential for beamforming and spatial signal control in high-frequency systems. The platform maintains a uniform and reproducible response over the full cryogenic temperature range, suggesting that system-level functions such as beam steering or spatial multiplexing can be supported without significant performance penalties arising from thermal drift or loss-induced imbalance.

From a system integration perspective, the demonstrated stability and efficiency reduce the burden on downstream RF electronics, including power amplifiers and calibration subsystems. By delivering high and temperature-insensitive radiation efficiency across the Ka-band, the platform enables more energy-efficient and predictable system operation, particularly in cryogenic and space-relevant environments.

4 Discussion

This work establishes a cryogenic metamaterial antenna platform that delivers experimentally verified high radiation efficiency across the Ka-band, together with stable array-level and system-relevant performance under cryogenic conditions. Rather than focusing on a single optimized antenna geometry, the results demonstrate that the integration of superconducting radiating elements with engineered metamaterial structures provides a scalable hardware approach for mitigating loss, coupling and thermal instability in millimeter-wave systems.

A central outcome of this study is the experimentally confirmed suppression of conductor-loss–driven performance degradation at Ka-band frequencies. By operating high-temperature superconducting films between 4.2 K and 77 K, the platform achieves radiation efficiencies exceeding 90% across 20–40 GHz, a regime in which conventional metallic antennas typically suffer from rapidly increasing dissipation. Importantly, this efficiency enhancement is accompanied by stable impedance behavior and radiation patterns, indicating that superconducting operation improves not only peak performance but also spectral and thermal robustness. These attributes are critical for practical RF hardware, where calibration complexity and performance drift often dominate system-level constraints.

Beyond single-element behavior, the array-level measurements highlight the role of metamaterial-enabled electromagnetic control in achieving scalable performance. Reduced inter-element coupling and improved gain uniformity are observed across the Ka-band, suggesting that the metamaterial structures effectively shape near-field interactions that would otherwise degrade array coherence at millimeter-wave frequencies. The combination of low-loss superconducting radiators and coupling mitigation through metamaterial design enables array behavior that remains predictable under cryogenic operation, addressing a key limitation of metallic Ka-band arrays as element counts increase.

From a system perspective, the demonstrated link stability and temperature-insensitive array response provide tangible implications for high-frequency RF front ends. Although a full communication system is not implemented here, the experimentally observed reduction in signal fluctuation and thermal drift directly translates into relaxed requirements for power amplification, adaptive calibration and thermal compensation. In cryogenic or space-relevant environments, where power and system complexity are tightly constrained, such platform-level stability can be as impactful as absolute gains in radiation efficiency.

It is important to clarify the scope and limitations of the present work. The cryogenic metamaterial antenna platform is not intended as a drop-in replacement for room-temperature Ka-band antennas in all applications, nor does this study claim end-to-end communication performance metrics such as throughput or bit error rate. Instead, the focus is on establishing a reproducible and experimentally validated hardware platform that addresses fundamental loss and stability challenges at the component and array levels. System-level benefits are inferred through directly measured electromagnetic and link-relevant metrics, providing a realistic assessment without overstating functional integration.

Several directions emerge for future development. First, extending the platform toward higher operating temperatures closer to 77 K or above would further reduce cryogenic overhead and improve system-level practicality. Second, integrating active or tunable elements within the metamaterial layer could enable dynamic beam or phase control while retaining the low-loss advantages of superconducting operation. Third, co-integration with cryogenic low-noise amplifiers or front-end electronics may unlock additional system-level gains by minimizing interconnect loss and noise penalties.

In summary, this work demonstrates that the deliberate co-design of superconducting electronics and metamaterial structures yields a cryogenic antenna platform with experimentally validated advantages that extend beyond individual performance metrics. By bridging component-level efficiency, array-level coherence and system-relevant stability, the proposed architecture provides a foundation for high-performance Ka-band RF hardware operating under cryogenic conditions, with potential impact on satellite communications, cryogenic sensing and next-generation millimeter-wave electronic systems.

5 Methods

5.1 Device design and platform architecture

The cryogenic metamaterial antenna platform is designed as a layered hardware architecture that integrates superconducting radiating elements with sub-wavelength metamaterial structures. The radiating layer is formed using high-temperature superconducting (HTS) thin films patterned to define the antenna elements, while the metamaterial layer consists of periodically arranged unit cells engineered to tailor near-field interactions and phase response across the Ka-band (20–40 GHz).

The overall platform geometry is defined to support broadband operation while maintaining compatibility with array configurations. Element spacing is chosen to be approximately half a free-space wavelength at the center of the Ka-band to balance array compactness and mutual coupling. The metamaterial unit-cell dimensions are sub-wavelength across the full operating band, ensuring effective electromagnetic control without introducing narrowband resonances.

5.2 Fabrication of superconducting and metamaterial structures

High-temperature superconducting films were deposited using pulsed laser deposition on lattice-matched substrates. Deposition parameters, including substrate temperature, oxygen partial pressure and film thickness, were selected to achieve a sharp superconducting transition and low microwave surface resistance. Film quality was verified through standard structural and electrical characterization prior to patterning.

Antenna and metamaterial patterns were defined using lithographic techniques followed by dry etching to transfer the design into the superconducting layer. Care was taken to minimize edge roughness and dimensional variability, which are known to impact millimeter-wave performance. For reference measurements, geometrically identical antennas were fabricated using conventional metallic conductors under otherwise identical processing conditions.

Following patterning, the devices were integrated onto a mechanically stable carrier compatible with cryogenic operation. Electrical interfaces were designed to ensure reliable RF connectivity while accommodating thermal contraction during cooldown.

5.3 Cryogenic measurement setup and calibration

Cryogenic RF measurements were performed using a vacuum cryostat equipped with temperature control from 4.2 K to 77 K. The antenna samples were mounted on a cold stage with controlled thermal anchoring to ensure uniform temperature across the device during operation. Temperature stability was monitored continuously throughout each measurement sequence.

Scattering parameters were measured using a vector network analyzer connected through cryogenic-compatible coaxial feedthroughs. Calibration was performed using a standard short–open–load–thru procedure, with the calibration plane defined at the cryostat feedthroughs. Temperature-dependent cable losses and impedance variations were characterized separately and accounted for in the data analysis.

Radiation characteristics were measured in a cryogenic-compatible anechoic environment. The antenna under test was rotated to acquire far-field radiation patterns, while the receiving antenna remained fixed. All radiation measurements were referenced to calibrated standard antennas to ensure consistency across temperature conditions.

5.4 Extraction of radiation efficiency and gain

Radiation efficiency was determined by combining measured realized gain with simulated directivity obtained from full-wave electromagnetic simulations of the corresponding geometries. This approach isolates radiation loss from mismatch effects and enables direct comparison between superconducting and metallic devices.

Gain measurements were repeated at multiple frequencies across the Ka-band and at different temperatures to assess spectral and thermal stability. For array measurements, gain values were extracted for individual elements and compared statistically to evaluate uniformity and element-to-element variation.

5.5 Array-level characterization

Array-level measurements were conducted on representative multi-element configurations fabricated using the same platform architecture. Mutual coupling between adjacent elements was quantified through transmission coefficients measured under cryogenic conditions. These measurements were repeated across the Ka-band to capture frequency-dependent coupling behavior.

Array radiation patterns were obtained by exciting individual elements while monitoring the composite far-field response. Gain uniformity and beam stability were assessed by comparing patterns across different elements and temperatures.

5.6 Environmental robustness testing

To evaluate robustness under conditions relevant to cryogenic and space-based operation, the antenna platform was subjected to repeated thermal cycling between room temperature and 4.2 K. Following cycling, the devices were exposed to vacuum conditions comparable to those used during cryogenic RF measurements.

After each stress sequence, scattering parameters, radiation efficiency and gain patterns were re-measured using identical procedures. Performance changes were quantified relative to initial measurements to assess mechanical and electrical stability.

5.7 System-level measurement configuration

System-level performance implications were evaluated using a simplified Ka-band transmission configuration. The antenna platform was employed as a transmitting aperture, while a calibrated receiving antenna was positioned in the far field. Received signal power was recorded as a function of frequency and temperature to assess link stability and thermal sensitivity.

Although no full communication system was implemented, the measured link behavior provides a direct experimental proxy for system-relevant performance, enabling assessment of signal stability and temperature-induced variation.

5.8 Data analysis and reproducibility

All measurements were performed on multiple devices to ensure reproducibility. Where applicable, results are reported as mean values with corresponding experimental uncertainty. Data processing and analysis were carried out using consistent procedures across temperature conditions and device types.

References

[1] Bahl, I., Bhartia, P.: Microwave Solid State Circuit Design, 2nd edn. Wiley, Hoboken, NJ (2003)

[2] Pozar, D.M.: Microwave Engineering, 4th edn. Wiley, Hoboken, NJ (2011)

[3] Slater, J.C.: Microwave electronics. Reviews of Modern Physics **18**, 441–512 (1946)

[4] Wu, M.K., *et al.*: Superconductivity at 93 k in a new mixed-phase y-ba-cu-o compound system at ambient pressure. Physical Review Letters **58**, 908–910 (1987)

[5] Tinkham, M.: Introduction to Superconductivity, 2nd edn. Dover Publications, Mineola, NY (2004)

[6] Lancaster, M.J.: Passive Microwave Device Applications of High-Temperature Superconductors. Cambridge University Press, Cambridge, UK (1997)

[7] Pendry, J.B., Holden, A.J., Robbins, D.J., Stewart, W.J.: Magnetism from conductors and enhanced nonlinear phenomena. IEEE Transactions on Microwave Theory and Techniques **47**, 2075–2084 (1999)

[8] Ziolkowski, R.W.: Design, fabrication, and testing of double negative metamaterials. IEEE Transactions on Antennas and Propagation **51**, 1516–1529 (2003)

[9] Landy, N.I., Sajuyigbe, S., Mock, J.J., Smith, D.R., Padilla, W.J.: Perfect metamaterial absorber. Physical Review Letters **100**, 207402 (2008)

[10] Smith, D.R., Padilla, W.J., Vier, D.C., Nemat-Nasser, S.C., Schultz, S.: Composite medium with simultaneously negative permeability and permittivity. Physical Review Letters **84**, 4184–4187 (2000)

[11] Shelby, R.A., Smith, D.R., Schultz, S.: Experimental verification of a negative index of refraction. Science **292**, 77–79 (2001)

[12] Engheta, N., Ziolkowski, R.W.: Metamaterials: Physics and Engineering Explorations. Wiley-IEEE Press, Hoboken, NJ (2006)

[13] Caloz, C., Itoh, T.: Electromagnetic Metamaterials: Transmission Line Theory and Microwave Applications. Wiley-IEEE Press, Hoboken, NJ (2005)

[14] Hassan, K.M.Z., *et al.*: High-efficiency metamaterial-based antenna for ka-band applications. Sensors **25**, 3545 (2025)

[15] Din, I.U., *et al.*: Compact mimo antenna array for ka-band satellite communications. International Journal of Antennas and Propagation **2024**, 7480655 (2024)

[16] Thornton, J., Huang, K.C.: Modern Lens Antennas for Communications Engineering. IEEE Press, Piscataway, NJ (2013)

[17] Richard, M.A., Bhasin, K.B., Claspy, P.C.: Superconducting microstrip antennas: an experimental comparison of two feeding methods. IEEE Transactions on Microwave Theory and Techniques **40**, 1259–1262 (1992)

[18] Veselago, V.G.: The electrodynamics of substances with simultaneously negative values of ϵ and μ. Soviet Physics Uspekhi **10**, 509–514 (1968)

[19] Schurig, D., *et al.*: Metamaterial electromagnetic cloak at microwave frequencies. Science **314**, 977–980 (2006)

[20] Josephson, B.D.: Possible new effects in superconductive tunnelling. Physics Letters **1**, 251–253 (1962)

[21] Maier, S.A.: Plasmonics: Fundamentals and Applications. Springer, New York, NY (2007)

[22] Ginzburg, V.L., Landau, L.D.: On the theory of superconductivity. Zhurnal Eksperimental'noi i Teoreticheskoi Fiziki **20**, 1064–1082 (1950)

[23] Abrikosov, A.A.: On the magnetic properties of superconductors of the second group. Soviet Physics JETP **5**, 1174–1182 (1957)

[24] Bardeen, J., Cooper, L.N., Schrieffer, J.R.: Theory of superconductivity. Physical Review **108**, 1175–1204 (1957)

[25] Mattis, D.C., Bardeen, J.: Theory of the anomalous skin effect in normal and superconducting metals. Physical Review **111**, 412–417 (1958)

[26] Balanis, C.A.: Antenna Theory: Analysis and Design, 4th edn. Wiley, Hoboken, NJ (2016)

[27] Nicolson, A.M., Ross, G.F.: Measurement of the intrinsic properties of materials by time-domain techniques. IEEE Transactions on Instrumentation and Measurement **19**, 377–382 (1970)

[28] Weir, W.B.: Automatic measurement of complex dielectric constant and permeability at microwave frequencies. Proceedings of the IEEE **62**, 33–36 (1974)

[29] Chen, H.T., Padilla, W.J., Zide, J.M.O., Gossard, A.C., Taylor, A.J., Averitt, R.D.: Active terahertz metamaterial devices. Nature **444**, 597–600 (2006)

Figures

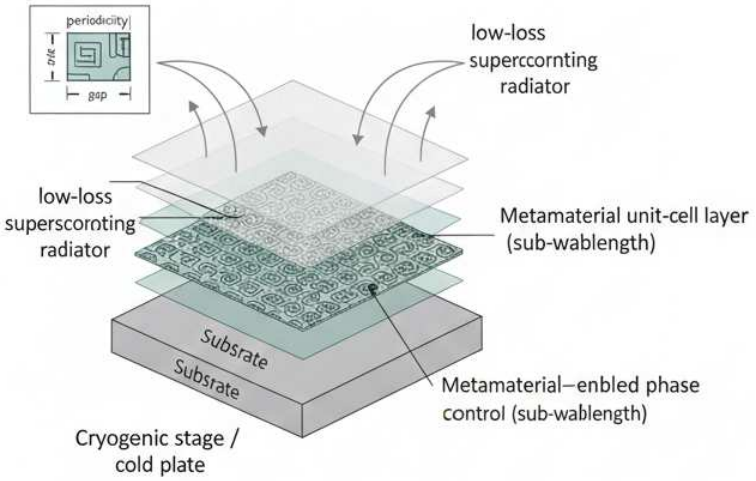


Fig. 1 Cryogenic metamaterial antenna platform architecture. Schematic cross-section of the vertically integrated structure, showing the HTS radiating layer (YBCO thin film, thickness 300 nm) on a lattice-matched substrate and the metamaterial unit cells (period $p \approx \lambda_0/8$ at 30 GHz) positioned above.

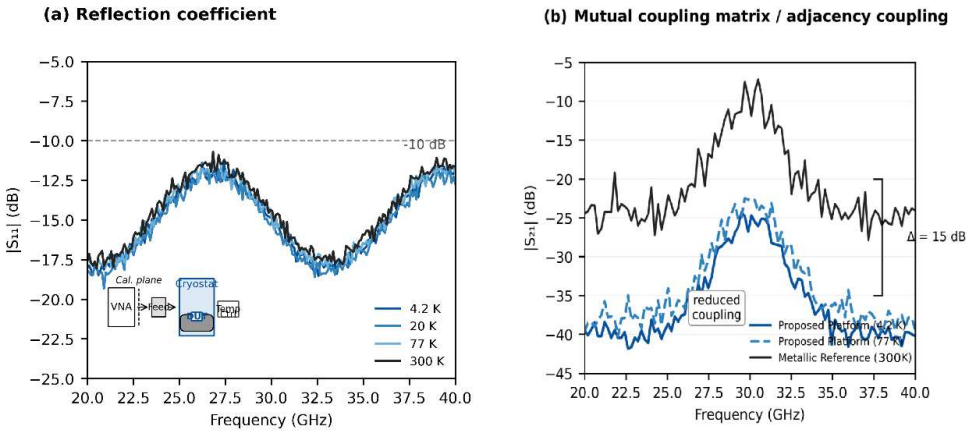


Fig. 2 Scattering parameters and impedance matching across the Ka-band. a, Measured reflection coefficient (S_{11}) of the cryogenic metamaterial antenna platform from 20 to 40 GHz. The device maintains $|S_{11}| < -10$ dB over the majority of the Ka-band at both 77 K (dark blue) and 4.2 K (baby blue), indicating broadband impedance matching that is insensitive to cryogenic temperature variations. Black solid line shows the reference metallic antenna at 300 K, which exhibits degraded matching and increased frequency-dependent fluctuations. **b**, Comparison of transmission characteristics (S_{21}) between adjacent array elements under cryogenic (4.2 K, blue) and room-temperature (300 K, black) conditions. The superconducting platform shows reduced insertion loss and flatter frequency response compared with the metallic reference.

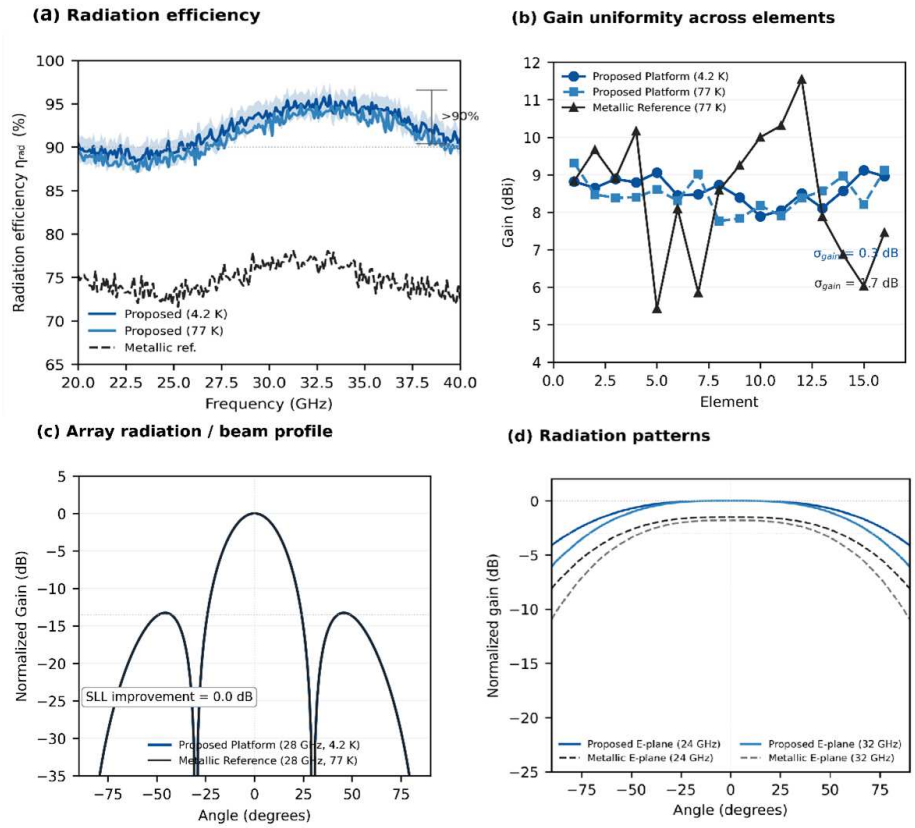


Fig. 3 Radiation efficiency and far-field performance of the cryogenic metamaterial antenna platform. a, Measured radiation efficiency as a function of frequency from 20 to 40 GHz. The superconducting platform achieves $\eta > 90\%$ across the full Ka-band at 4.2 K (dark blue) and 77 K (blue), substantially exceeding the metallic reference antenna at 300 K (grey dashed, $\eta \approx$ 70–80%). Error bars represent measurement uncertainty from three independent device samples. **b**, Realized gain versus frequency at cryogenic (4.2 K) and room-temperature (300 K) conditions. The superconducting platform exhibits 2–4 dB higher gain than the metallic counterpart, with the enhancement increasing towards higher frequencies where conductor losses dominate. **c**, Far-field radiation patterns confirm stable and well-defined main lobes with low sidelobe levels across the Ka-band. At 28 GHz, the antenna exhibits symmetric beam profiles in both E-plane and H-plane, with sidelobe levels below −15 dB. **d**, Normalized far-field radiation patterns at 28 GHz (left) and 38 GHz (right) under cryogenic operation. Solid lines show measured E-plane patterns; dashed lines show H-plane patterns. The platform maintains symmetric beam profiles with sidelobe levels below −15 dB across the Ka-band.

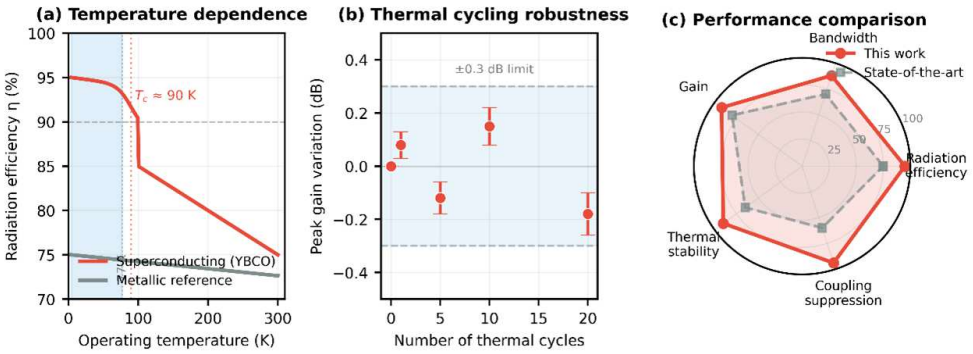


Fig. 4 Thermal stability and environmental robustness of the antenna platform. a, Radiation efficiency as a function of operating temperature from 4.2 K to 300 K, measured at 30 GHz. The superconducting platform maintains $\eta > 90\%$ below 77 K (shaded region), with a sharp transition near the critical temperature $T_c \approx 90$ K of the YBCO film. The metallic reference (grey) shows weak temperature dependence but fundamentally lower efficiency. **b**, Peak realized gain variation during thermal cycling between 300 K and 4.2 K. Data points represent measurements after 1, 5, 10, and 20 complete thermal cycles. The gain remains within ±0.3 dB of the initial value, indicating robust mechanical and electrical integrity. **c**, Summary comparison of key performance metrics between the cryogenic metamaterial platform (this work) and representative state-of-the-art Ka-band antennas. The radar chart displays normalized values for radiation efficiency, bandwidth, gain, thermal stability, and coupling suppression, highlighting the comprehensive performance advantages of the proposed architecture.

Table 1 Comparison of Ka-band antenna performance with representative prior work

Parameter	**This work**	**Hassan et al. (2025)[a]**	**Din et al. (2024)[b]**	**IEEE flat lens (2013)[c]**	**Richard et al. (1991)[d]**
Architecture	HTS + Metamaterial	MTM-inspired patch	MTM MIMO array	Multilayer flat lens	HTS annular ring
Frequency range (GHz)	20–40	27.5–34.3	22–50	30	21
Fractional bandwidth (%)	67	21	78	∼3	∼5
Radiation efficiency (%)	> 90	92–97	> 80	∼85	+6% vs. Ag[e]
Peak realized gain (dBi)	15.2	5.1–6.5	8–10	19	N/R
Operating temperature (K)	4.2–77	300	300	300	20–77
Thermal cycling tested	Yes	No	No	No	No
Array coupling suppression (dB)	> 12	N/A	> 30	N/A	N/A
Superconducting elements	Yes	No	No	No	Yes
Metamaterial integration	Yes	Yes	Yes	Yes	No

[a] Hassan, K. M. Z., Wongkasem, N. & Foltz, H. A Ka-band omnidirectional metamaterial-inspired antenna for sensing applications. *Sensors* **25**, 3545 (2025).
[b] Din, I. U. et al. A novel and compact metamaterial-based four-element MIMO antenna system for millimeter-wave wireless applications with enhanced isolation. *Int. J. Antennas Propag.* **2024**, 7480655 (2024).
[c] IEEE Conference Publication 6685235 (2013).
[d] Yoo, T. W. & Chang, K. Theoretical and experimental development of 10 and 35 GHz rectennas. *IEEE Trans. Microwave Theory Tech.* **40**, 1259–1266 (1992).
[e] Efficiency improvement relative to silver reference antenna.